

# A Guide to Differences between Stochastic Point-Source and Stochastic Finite-Fault Simulations

by Gail M. Atkinson, Karen Assatourians, David M. Boore, Ken Campbell, and Dariush Motazedian

**Abstract** Why do stochastic point-source and finite-fault simulation models not agree on the predicted ground motions for moderate earthquakes at large distances? This question was posed by Ken Campbell, who attempted to reproduce the [Atkinson and Boore \(2006\)](#) ground-motion prediction equations for eastern North America using the stochastic point-source program SMSIM ([Boore, 2005](#)) in place of the finite-source stochastic program EXSIM ([Motazedian and Atkinson, 2005](#)) that was used by [Atkinson and Boore \(2006\)](#) in their model. His comparisons suggested that a higher stress drop is needed in the context of SMSIM to produce an average match, at larger distances, with the model predictions of [Atkinson and Boore \(2006\)](#) based on EXSIM; this is so even for moderate magnitudes, which should be well-represented by a point-source model. Why?

The answer to this question is rooted in significant differences between point-source and finite-source stochastic simulation methodologies, specifically as implemented in SMSIM ([Boore, 2005](#)) and EXSIM ([Motazedian and Atkinson, 2005](#)) to date. Point-source and finite-fault methodologies differ in general in several important ways: (1) the geometry of the source; (2) the definition and application of duration; and (3) the normalization of finite-source subsurface summations. Furthermore, the specific implementation of the methods may differ in their details. The purpose of this article is to provide a brief overview of these differences, their origins, and implications. This sets the stage for a more detailed companion article, “Comparing Stochastic Point-Source and Finite-Source Ground-Motion Simulations: SMSIM and EXSIM,” in which [Boore \(2009\)](#) provides modifications and improvements in the implementations of both programs that narrow the gap and result in closer agreement. These issues are important because both SMSIM and EXSIM have been widely used in the development of ground-motion prediction equations and in modeling the parameters that control observed ground motions.

## Introduction

This article was motivated by a question asked by Ken Campbell to the rest of us: Why is it that we cannot approximately reproduce the stochastic simulations of [Atkinson and Boore \(2006\)](#) for eastern North America, which were made with the finite-fault stochastic model EXSIM ([Motazedian and Atkinson, 2005](#)), by using the point-source stochastic model SMSIM ([Boore, 1983, 2005](#)), with the same model parameters? Specifically, it appears that a stress drop of about 250 bars is needed in SMSIM to approximately match the predictions of [Atkinson and Boore \(2006\)](#), which were based on EXSIM with 140 bars, when all other model parameters are set to be equal (see [Campbell, 2008](#)). These other parameters, describing regional physical constants, attenuation, and path-duration, are listed in [Atkinson and Boore \(2006\)](#). This is true

even for moderate-magnitude events at large distances, which should behave as point sources. Should not point-source and finite-fault stochastic simulations provide the same predicted ground motions for moderate earthquakes, and at large distances, if the input parameters are the same?

Answering this question is the purpose of this article. It proved to be more difficult than anticipated, and led to significant proposed changes in the way that both finite-fault and point-source stochastic models are implemented ([Boore, 2009](#)) that bring the approaches closer together. This article focuses on the specific point-source stochastic implementation of SMSIM and the finite-fault stochastic implementation of EXSIM, because both of these programs are freely available and have been widely used in a variety of applications

(many of which have been published in *BSSA*). However, many of the issues discussed are generic, and apply to point-source and finite-fault simulation methods in general, particularly those that employ a stochastic approach (either wholly or partly).

Both EXSIM and SMSIM are based on a stochastic simulation approach in which the motions are treated as a random Gaussian signal (white noise) superimposed on an underlying Brune-model source spectrum, characterized by its stress drop parameter (see [Hanks and McGuire, 1981](#); [Boore, 1983](#); [Atkinson and Boore, 1995, 1997](#); [Toro et al., 1997](#); [Atkinson and Beresnev, 1997](#); [Atkinson and Silva, 2000](#); [Boore, 2003](#); [Motazedian and Atkinson, 2005](#); [Atkinson and Boore, 2006](#)). However, there are a number of important differences in approach between the EXSIM and SMSIM programs that can lead to significant differences in predicted ground motions. Some of these are inherent differences between point-source and finite-fault approaches, and some are due to specific choices made in model implementation. In this article, we overview the differences between the EXSIM and SMSIM methodologies as implemented to date, and illustrate their net consequences with an example. This sets the stage for a companion article by [Boore \(2009\)](#), which presents modifications or improvements that can be made in the implementation of both programs that narrow the gap in methodologies and result in closer agreement. The work also provides the backdrop for a new hybrid empirical ground-motion model for eastern North America (ENA), currently under revision by Campbell (unpublished manuscript).

The issues raised here are important because both EXSIM and SMSIM have been widely used in the development of ground-motion prediction equations and in modeling the parameters that control observed ground motions. Thus, an understanding of differences in meaning of the parameters used in these programs (as implemented to date) is useful in interpretation of studies based on point-source or finite-source stochastic models. Although this article focuses on the SMSIM and EXSIM programs, the concepts are general and may apply to other point-source or finite-source programs as well.

### Background to the Question Posed

[Atkinson and Boore \(2006\)](#) developed ground-motion prediction equations for eastern North America (ENA) based on the stochastic finite-source model of [Motazedian and Atkinson \(2005\)](#), as implemented in the program EXSIM. The stochastic finite-source model used in [Atkinson and Boore \(2006\)](#) subdivides a finite source into sub-sources. Each sub-source is treated as a stochastic point source with an underlying spectrum as given by the Brune point source, with a stress drop parameter of 140 bars. The modeling of sub-sources in EXSIM closely follows the point-source stochastic model developed by [Boore \(1983, 2000\)](#), and popularized by the SMSIM computer code ([Boore, 2000, 2003, 2005](#)). In [Atkinson and Boore \(2006\)](#), the attenuation from

sub-sources to sites is specified using the ENA attenuation model of [Atkinson \(2004\)](#). The duration of motion comes from the source duration plus the path duration, where the path component uses, for each sub-source, the distance-dependent duration model proposed by [Atkinson and Boore \(1995\)](#).

The 140-bar stress parameter used in [Atkinson and Boore \(2006\)](#) was derived by comparing the high-frequency spectral levels of ENA earthquakes that were inferred for near-source distances with those predicted by EXSIM for various levels of stress. Thus, the 140-bar stress used in [Atkinson and Boore \(2006\)](#) effectively calibrated the EXSIM model to the ENA observational database. Last year, while working on revisions to his Hybrid Empirical ENA ground-motion model, Ken Campbell attempted to reproduce the [Atkinson and Boore \(2006\)](#) ground-motion predictions for ENA with SMSIM, using the same source, attenuation, and duration parameters that were specified in [Atkinson and Boore \(2006\)](#). However, he found that the motions he predicted using SMSIM were significantly lower than those given in [Atkinson and Boore \(2006\)](#). When he doubled the stress drop value (e.g., 280 bars input to SMSIM, in comparison to 140 bars input to EXSIM for [Atkinson and Boore, 2006](#)), he then predicted motions similar to those of [Atkinson and Boore \(2006\)](#), at least at large distances ([Campbell, 2008](#)). This raised the question addressed in this article: Why do EXSIM and SMSIM not agree? In order to understand the answer to this question, we first overview the basics of stochastic point-source and finite-fault modeling.

### Stochastic Point-Source Modeling

The stochastic point-source model assumes that the source is concentrated at a point, and that the acceleration time series generated at a site carry both deterministic and random aspects of ground-motion shaking. The deterministic aspects are specified by the average Fourier spectrum, typically as a function of magnitude and distance. The stochastic aspects are treated by modeling the motions as noise with the specified underlying spectrum. The point-source assumption is reasonable when the source-to-site distance is much larger than the source dimensions ([Boore, 1983, 2003](#); [Boore and Atkinson, 1987](#); [Atkinson and Boore, 1995, 1997](#); [Atkinson and Silva, 1997, 2000](#)). The steps of synthesizing ground motions using the stochastic point-source model are ([Boore, 2003](#)):

1. Generate a normally distributed random signal having zero mean and unit variance.
2. Window the signal by multiplying it by a window function.
3. Calculate the Fourier transform of the windowed signal.
4. Normalize the result so that the RMS amplitude spectrum equals unity.
5. Calculate the theoretical (deterministic) point-source spectrum. The total point-source spectrum is calculated by the following equation:

$$\text{Acc}(M_0, R, f) = \text{Source}(M_0, f)\text{Path}(R, f)\text{Site}(f), \quad (1)$$

where  $\text{Acc}(M_0, R, f)$  is total point-source spectrum observed at recording site;  $\text{Source}(M_0, f)$  is the source spectrum at unit distance;  $\text{Path}(R, f)$  is the path effect that includes the effects of both geometrical spreading and inelastic attenuation;  $\text{Site}(f)$  is the site response operator that includes the effects of both site (de)amplification and the high-frequency deamplification (Hanks 1982; Anderson and Hough, 1984);  $M_0$  is seismic moment (Aki, 1967);  $R$  is the distance from the source to site; and  $f$  is the frequency.

6. Multiply equation (1) by the normalized random-signal complex spectrum to obtain the Fourier spectrum of the motion at the site.
7. Calculate the inverse Fourier transform of the site spectrum to obtain the simulated accelerogram.

### Stochastic Finite-Source Modeling

There are important factors that influence the ground motions from large earthquakes that are not included in the stochastic point-source model, such as the effects of faulting geometry, distributed rupture, and rupture inhomogeneity. To consider these finite-fault effects in ground-motion modeling, Hartzell (1978) proposed subdividing the fault surface of an earthquake into a grid of subsources, each of which could be treated as a point source. The contributions to ground motion can be summed at the observation site, over all of the subsources comprising the fault, considering proper delays of subsources due to rupture propagation. This basic idea has been implemented in many articles (Irikura, 1983, 1992; Irikura and Kamae, 1994; Bour and Cara, 1997). To implement the concept for the stochastic approach to ground-motion modeling, Beresnev and Atkinson (1998a) discretized the fault into subsources and applied  $\omega^2$  stochastic point sources to each of the subsource activations, using the approach of Boore (2003, 2005) to generate the motion for each subsource (in fact, much of the FORTRAN code SMSIM was also adopted in the application). The properly delayed subsource effects are added in the time domain to generate the motion at an observation point. The stochastic finite-source code of Beresnev and Atkinson (1997, 1998a) was named FINSIM. Motazedian and Atkinson (2005) made a major modification to FINSIM to introduce the concept of dynamic corner frequency (Motazedian, 2002; Motazedian and Atkinson, 2005), in order to overcome the main difficulties associated with the heavy dependence of the simulation results of FINSIM on subsource size. The new approach also eliminated the need for multiple triggering of subevents. The new code, EXSIM, shows little dependence on subsource size under a range of conditions, as demonstrated by Motazedian and Atkinson (2005). However, it is not entirely free of subsource dependence, as discussed in the companion article by Boore (2009). In addition to introducing the concept of dynamic corner frequency, EXSIM also aimed to conserve

energy in the subsource summation, through a summation formulation that was based on normalization of the velocity spectrum.

It should be noted that there was a typographical error in equation (7) in Motazedian and Atkinson (2005) that carried through to the equation providing the normalization factor (equation 10). The actual implemented normalization factor ( $H_{ij}$ ) in EXSIM, based on the velocity spectrum, is:

$$H_{ij} = \left( N \sum \{f/[1 + (f/f_0)^2]\}^2 / \sum \{f/[1 + (f/f_{0ij})^2]\}^2 \right)^{1/2}. \quad (2)$$

In Motazedian and Atkinson (2005), each subsource is activated once with an appropriate delay time of  $\Delta t_i$ . For each activation, a stochastic point-source waveform with an underlying  $\omega^2$  source spectrum is generated. Properly normalized and delayed subsource contributions are summed in the time domain as:

$$\text{Acc}_{\text{tot}}(t) = \sum_{i=1}^N H_i \times \text{Acc}(t - \Delta t_i - T_i), \quad (3)$$

where  $\text{Acc}_{\text{tot}}(t)$  is the total seismic signal at site;  $H_i$  is a normalization factor for the  $i$ th subsource that aims to conserve energy;  $\text{Acc}(t)$  is the signal of  $i$ th subsource activation (inverse Fourier of combined effects of noise spectrum and equation 1);  $N$  is the total number of subsources;  $\Delta t_i$  is delay time of the subsource; and  $T_i$  is a fraction of rise time. The rise time of each subsource in EXSIM is based on the subfault radius divided by the rupture velocity, while the total time of radiation from the source will be controlled by the time required for rupture propagation along the length of the fault, as each subsource ruptures in turn and is then delayed accordingly in its arrival at the observation point. The duration of radiation from the source in EXSIM does not depend explicitly on the stress parameter, but may be implicitly dependent on the stress parameter if fault size depends on stress drop. For example, in Atkinson and Boore (2006), small faults were specified for ENA due to the high stress drop, thus resulting in relatively short source durations. In general the treatment of source effects in EXSIM, FINSIM, and SMSIM is simplistic and does not include the possible effects of factors such as source mechanism, depth, and so on, except indirectly through the ability to vary the stress parameter.

Since their development, the programs SMSIM, FINSIM, and EXSIM have been publicly distributed free of charge, and used in a host of applications, ranging from development of ground-motion prediction equations to the estimation of underlying model parameters for observed ground motions. In this article, we focus on the comparison between SMSIM and EXSIM, because EXSIM has superseded FINSIM. For the comparisons, we consider the source, path, and site

parameters for ENA used in the ground-motion prediction equations of [Atkinson and Boore \(2006\)](#) for hard-rock sites. The source and path parameters are listed in Table 1; the site amplification factors are listed in Table 2.

### The Answer to the Question: Why Do EXSIM and SMSIM Not Predict the Same Motions?

There are several reasons why EXSIM and SMSIM (as implemented to date) do not predict the same ground-motion amplitudes for the same source and attenuation input parameters. Some of these come from basic differences between the methodologies. In stochastic point-source modeling, the geometry is a point, and the distance measure from the source is typically hypocentral distance ([Boore, 2009](#) discusses alternative distance definitions in the companion article). In stochastic finite-source modeling, the geometry is a plane, and the distance from the observation point to the source will be different for each subsource. The overall distance in EXSIM is typically summarized by the closest distance to the fault for the purposes of providing a single metric for the development of ground-motion prediction equations; however, because the total motion is computed as a summation over the subfaults, the overall distance may also be viewed as an average of the subfault-site distances. Thus, the distance measures in SMSIM and EXSIM will only be equivalent for moderate events at large distances. In a general case, the difference in geometry will result in different average source-to-site distances for the two approaches. Thus, when

Table 1

Source and Path Parameters of [Atkinson and Boore \(2006\)](#) ENA Model Implemented in Simulations\*

Parameter	Median Value
Shear-wave velocity (at 13 km depth) ( $\beta$ )	3.7 km/sec
Density (at 13 km depth)	2.8 g/cm <sup>3</sup>
*Rupture propagation speed	0.8 $\beta$
Stress parameter	140 bars
*Pulsing percentage	50%
Kappa	0.005
Geometric spreading $R^b$ : $b =$	-1.3 (0–70 km) +0.2 (70–140 km) -0.5 (> 140 km)
Distance dependence of duration, $d R$ , $d =$	0.0 (0–10 km) +0.16 (10–70 km) -0.03 (70–130 km) +0.04 (> 130 km)
Quality factor	$Q = \max(1000, 893f^{0.32})$
*Slip distribution and hypocenter location	Random
*Fault dip	90°
*Fault length and width	<b>M5</b> : 3.6 km × 1.2 km <b>M7</b> : 29.4 km × 9 km
*Fault subdivision into subsources	<b>M5</b> : 3 × 1 <b>M7</b> : 15 × 4

\*The parameters marked \* correspond specifically to the stochastic finite-fault modeling in EXSIM, while other parameters are used in both EXSIM and SMSIM.

Table 2

Site Amplification Factors for Hard-Rock Site Implemented in the Simulations

Frequency (Hz)	Amplification Factor
0.5	1.00
1	1.13
2	1.22
5	1.36
10	1.41
50	1.41

comparing finite-fault and point-source simulations, we should expect differences in predicted ground motions that are attributable to the different effective distances at which the source is located relative to the observation point. [Boore \(2009\)](#) discusses this point more quantitatively.

The difference in geometry also has a significant impact on duration. In SMSIM, the duration is specified as the source duration, which is based on event corner frequency, plus a distance-dependent distance term. In EXSIM, the total time of radiation from the source will be controlled largely by the time required for rupture propagation along the length of the fault, as each subsource ruptures in turn and is then delayed accordingly in its arrival at the observation point. Additionally, in EXSIM each subsource has a distance-dependent duration term that is added at the observation point, but delayed according to the propagation effects. Thus, the total duration of motion at the observation point may be very different for EXSIM than for SMSIM (though the durations can be made similar through appropriate choices of simulation parameters). Differences in duration can result in different response spectral amplitudes. In general, a shorter duration will result in higher response spectral amplitudes for the same underlying Fourier spectrum.

The stress drop parameter that controls the strength of the high-frequency radiation does not actually have the same meaning in EXSIM and SMSIM. In SMSIM, it comes directly from the Brune source model for a given stress parameter, in which the stress drop, corner frequency, and seismic moment control the spectral amplitudes (see [Boore, 2003](#) for details). However, in EXSIM, it has this meaning only for a particular subsource. The summation over the subsources was based on an algorithm that normalizes the high-frequency spectra to the appropriate level for the specified stress drop, using normalization of velocity spectra to conserve energy ([Mottazedian and Atkinson, 2005](#)). The value of the stress drop parameter in EXSIM is thus not directly comparable to that in SMSIM, though as [Boore \(2009\)](#) shows in the companion article, the results of EXSIM and SMSIM can be made much more similar if the EXSIM normalization is based on the acceleration spectrum rather than the velocity spectrum. [Boore \(2009\)](#) recommends the use of the acceleration spectrum for the normalization, partly for this reason, but the overall choice between velocity or acceleration normalization is largely a matter of convention. Any normalization method

might be chosen so long as the underlying parameters (and in particular the stress parameter) are consistently calibrated against the data. The normalization method turns out to be a very important factor controlling differences in predicted motions from EXSIM and SMSIM at high frequencies, and is the principal reason why a higher stress parameter needs to be used with SMSIM to make the simulated motions agree with the [Atkinson and Boore \(2006\)](#) predictions for ENA.

Finally, in the course of investigating the differences between EXSIM and SMSIM, we found that there are some deficiencies in the EXSIM modeling assumptions that affect low-frequency motions in EXSIM, as discussed in the modifications put forward by [Boore \(2009\)](#) in the companion article. These deficiencies arise chiefly from incoherent summation of low-frequency motions in EXSIM, which are exacerbated by a lack of zero-padding in the summation of subsource time series. The limitations in the modeling of low frequencies in EXSIM are the principal reason for the differences observed between SMSIM and EXSIM at low frequencies. Despite the limitations of EXSIM in its treatment of low frequencies, it should be noted that previous calibrations of EXSIM to observations from large earthquakes in California ([Motazedian and Atkinson, 2005](#)) and Japan ([Macias et al., 2008](#); [Atkinson and Macias, 2009](#)), and to moderate earthquakes in ENA ([Atkinson and Boore, 2006](#)), have not indicated any bias in the EXSIM model simulations at low frequencies. As reported in these articles, EXSIM simulations match observations well over a range of frequencies from 0.2 to 20 Hz. Nevertheless, it is important to recognize that although we may be able to show that data are consistent with a model, we cannot use data to prove that a model is accurate.

An example of the net effect of differences between SMSIM and EXSIM is provided in [Figure 1](#). To overview the effects for a range of magnitudes and distances, the geometric mean response spectra (PSA, 5% damped pseudoacceleration, for the random horizontal component of motion) from 100 SMSIM and 100 EXSIM simulations are compared for **M5** and **M7** earthquakes, at a hypocentral distance (SMSIM) or closest distance to the fault (EXSIM) of 15 km and 200 km; for the EXSIM simulations the sites are placed on a racetrack around the fault at the specified distance. This allows azimuthal averaging of results over a number of site-source geometries at the given distance. It should be noted that the distance measures for SMSIM and EXSIM (hypocentral and closest distance to the fault, respectively) are approximately equivalent for large distances (200 km), and for small magnitudes (**M5** at 15 km). For **M7** at 15 km, finite-fault effects result in a significant difference in meaning between point-source and finite-fault distance measures. This difference is one of the reasons for differences in results as illustrated in this article. In the companion article, [Boore \(2009\)](#) outlines changes that can be made to the distance metric for point-source simulations to make them more equivalent to finite-fault distances. Both sets of simulations use the ENA hard-rock parameters of [Atkinson and Boore](#)

(2006), as given in [Tables 1 and 2](#). For the EXSIM simulations, the stress parameter of 140 bars was used as in [Atkinson and Boore \(2006\)](#). For SMSIM, results for two stress-parameter values are shown: 140 bars and 200 bars. These comparisons are made without implementing any of the changes in EXSIM or SMSIM methodology proposed by [Boore \(2009\)](#) in the companion article. Thus, we use the same basic EXSIM algorithm as was used for [Atkinson and Boore \(2006\)](#). Similarly, we use hypocentral distance with SMSIM rather than the improved effective distance measure proposed by [Boore \(2009\)](#) in the companion article.

It should be noted that although the methodology for the EXSIM simulations with 140 bars is the same as that used in [Atkinson and Boore \(2006\)](#), the mean average ground motions from the simulations will not exactly match those of the [Atkinson and Boore \(2006\)](#) model. This is because there are some subtle differences in the applications. In particular, the [Atkinson and Boore \(2006\)](#) simulations considered aleatory variability in each of the input parameters and, hence, predicted a cloud of PSA values, from which regression equations were subsequently derived. It can be seen in [Figure 1](#) that the resulting [Atkinson and Boore \(2006\)](#) equations tend to predict slightly higher motions than the corresponding EXSIM simulations for fixed parameter values, especially at larger distances.

It can be seen in [Figure 1](#) that the EXSIM and SMSIM simulations agree with each other at high frequencies at 15 km, for both **M5** and **M7**, when a stress drop of 140 bars is used for both. At low frequencies, the EXSIM and SMSIM PSA values may differ from each other anywhere from 0 to 30%, depending on magnitude and distance. Far away from the source, at 200 km, a higher stress drop of roughly 200 bars is needed with SMSIM to match the high-frequency level obtained for 140 bars using EXSIM. However, at 15 km, a stress drop of 200 bars with SMSIM would overpredict the EXSIM spectra. We again see some differences at low frequencies, though these are minor in this case. In [Figure 2](#), the accelerograms are shown from both simulation methods, for the 140-bar stress parameter. The difference in the character and duration of strong shaking between the simulations for large magnitudes is apparent, which is one reason for the observed differences in spectra (the other main reason is the different normalization of high-frequency amplitudes). It should be noted that the abrupt end of the SMSIM seismograms is the result of the simple boxcar window used in the simulations; a more realistic-looking time series may be obtained by using a more tapered window shape, but this has no significant influence on either spectral or peak amplitudes and is thus cosmetic.

Finally, in [Figure 3](#) we show the attenuation with hypocentral distance for **M5** and **M7** simulations for two sample frequencies based on SMSIM with two stress-parameter values (140 bars and 250 bars), in comparison to the attenuation of the [Atkinson and Boore \(2006\)](#) prediction equations with closest distance to fault. (The 250 bar value is chosen because it provides the best overall match of the EXSIM

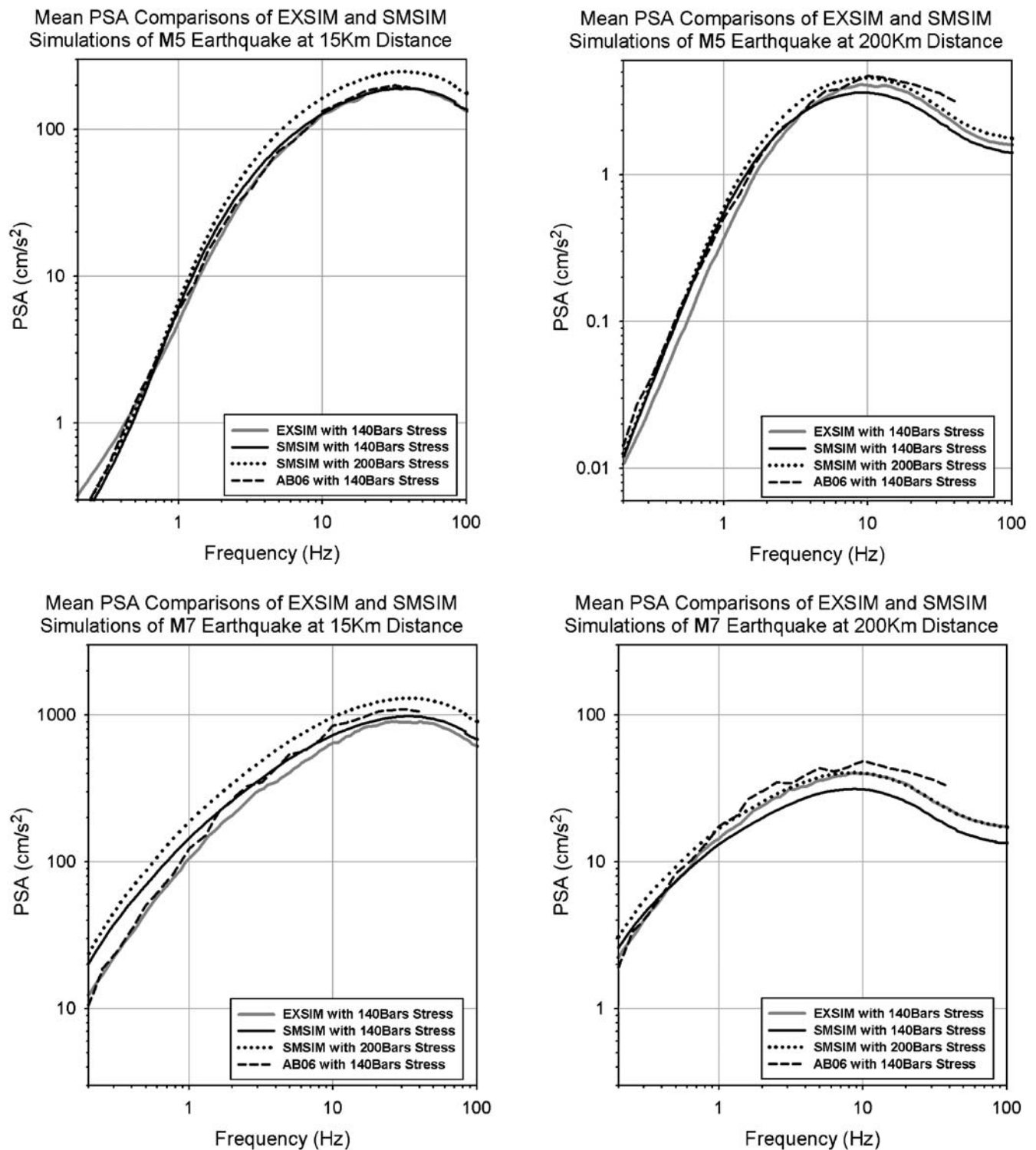


**Figure 1.** Comparison of the 5%-damped horizontal-component pseudoacceleration (PSA) for SMSIM (point-source) and EXSIM (finite-source) stochastic simulations of M5 and M7 earthquakes at 15 km and 200 km distances. The geometric mean for 100 simulations is shown in each case. The spectra from the prediction equations of [Atkinson and Boore \(2006\)](#) are also shown.

simulations with the revised code to the [Atkinson and Boore \[2006\]](#) equations.) The overall attenuation shape follows that determined empirically by [Atkinson \(2004\)](#), which was used in the [Atkinson and Boore \(2006\)](#) ground-motion simulation

model. It features relatively steep geometric spreading at distances less than 70 km, followed by a leveling in the 70–130 km distance range due to Moho bounce effects, then a gradual geometric spreading with significant anelastic

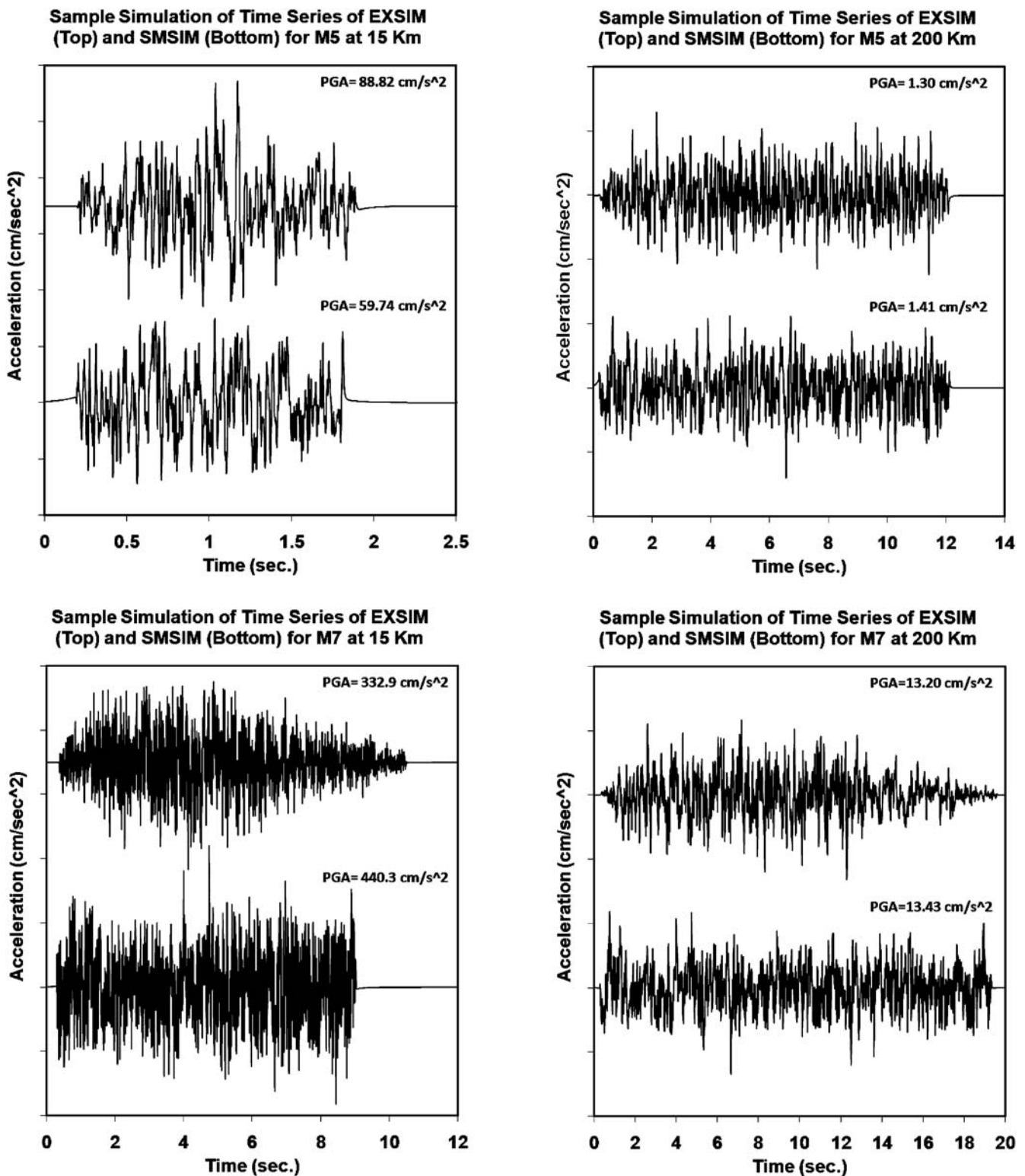


**Figure 2.** Comparison of sample horizontal-component acceleration time histories for SMSIM (point-source) and EXSIM (finite-source) stochastic simulations of M5 and M7 earthquakes at 15 km and 200 km distances. All simulations are for 140-bar stress parameter.

attenuation effects at larger distances. At close distances the [Atkinson and Boore \(2006\)](#) attenuation is less steep than that in SMSIM, due to finite-fault effects and the inherent differences in the distance measures used. At larger distances the

[Atkinson and Boore \(2006\)](#) equation values are close to those obtained with SMSIM using a stress drop value in the range from 140 to 250 bars, with the [Atkinson and Boore \(2006\)](#) curves tending toward the SMSIM predictions for 250 bars at

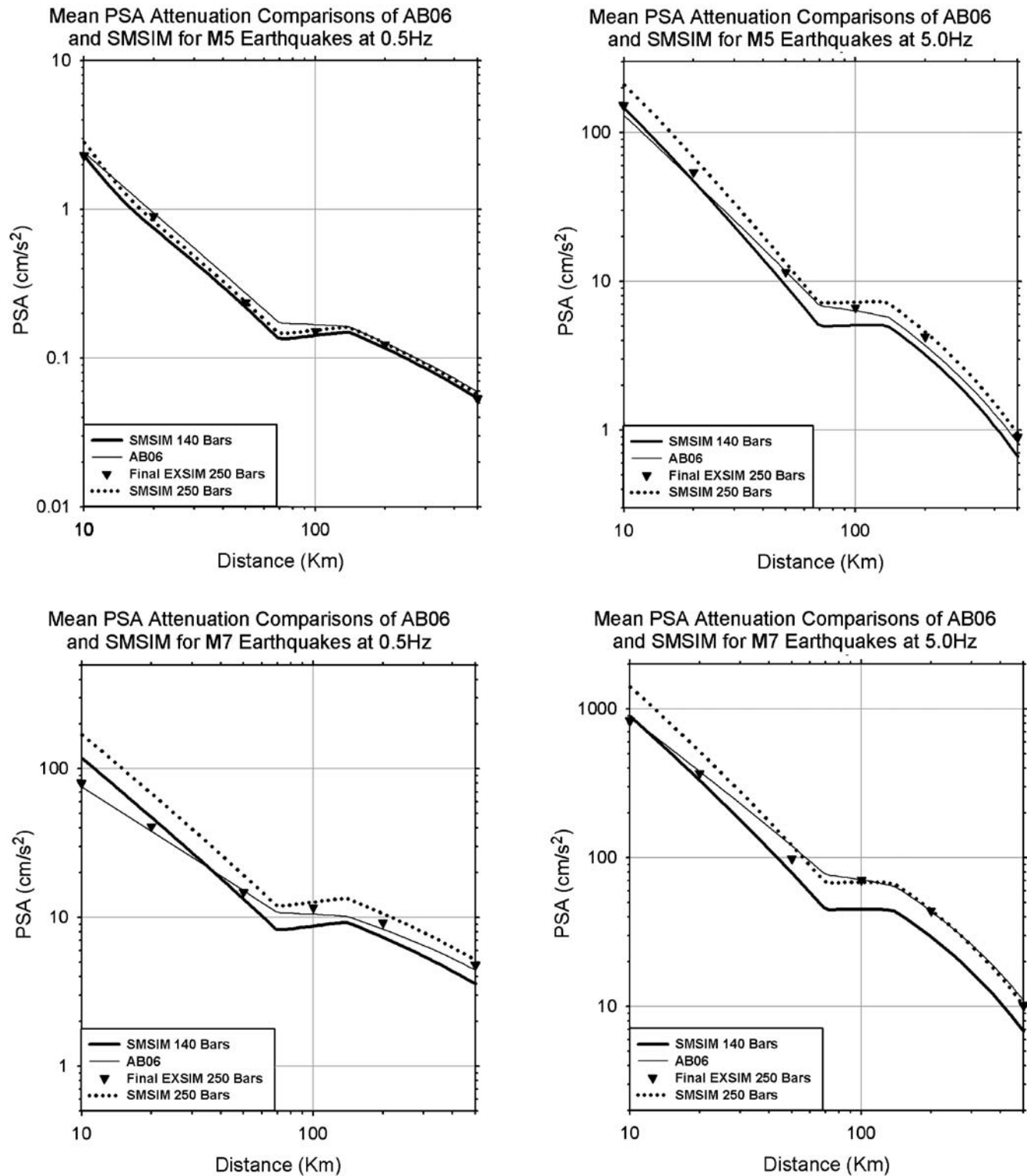


**Figure 3.** Attenuation of 5%-damped PSA (horizontal component) with distance for M5 and M7 simulated motions with SMSIM (140 and 250 bars), compared to Atkinson and Boore (2006) equations based on EXSIM simulations (140 bars). Distance measure is hypocentral for SMSIM, closest distance to the fault for Atkinson and Boore (2006). Also shown are EXSIM simulations for ENA made using the code improvements suggested by Boore (2009), for the median input parameter values used by Atkinson and Boore (2006), but using acceleration normalization in place of the velocity normalization, and therefore adjusting the stress drop to 250 bars to provide an approximate match to Atkinson and Boore (2006).

larger distances. To show the implications and effects of the changes in EXSIM proposed by Boore (2009) for the Atkinson and Boore (2006) equations, we also plot EXSIM simulations for ENA using the median parameter values from Atkinson and Boore (2006), calculated using the revised EXSIM code. In the revised code, the normalization is done on acceleration rather than velocity, and this necessitates a change in the median stress drop parameter. As shown in Figure 3, with the improved EXSIM code algorithm of Boore (2009), a stress drop of 250 bars for ENA provides a good overall match to the ground-motion predictions of Atkinson and Boore (2006). Figure 11 in Boore (2009) is similar to Figure 3, but shows that by using an effective distance rather than the closest distance in the SMSIM calculations, a much better match between SMSIM and EXSIM results at close distances may be achieved.

In summary, the differences in results obtained from the EXSIM and SMSIM simulations result from a complex interplay between the factors that differ between them: the geometry and distance measures, the origin of source and distance-dependent duration terms, and the approach to normalization of spectral summations in finite-fault modeling. Among these reasons, the way in which normalization of amplitudes is achieved at high and low frequencies in EXSIM is of particular importance, and was not appreciated prior to this article. The companion article by Boore (2009) expands on each of the reasons for the differences between EXSIM and SMSIM in more detail, and provides modifications to each that improve the programs and make them more comparable. The choice of which program to use depends on the application. The point-source approach (SMSIM) has the advantage of simplicity and can be manipulated to mimic the salient finite-fault effects by an appropriate modification to the distance measure; the finite-fault approach (EXSIM) is more flexible in modeling extended faults and exploring their effects on ground motions.

Finally, to avoid potential confusion, we wish to state clearly that the issues raised in this article do not significantly impact the published ground-motion prediction equations for ENA by Atkinson and Boore (2006). In particular, the issue of which normalization scheme is used (velocity or acceleration) is closely tied to the adopted value of stress drop. As we show in Figure 3, the adopted value of 140 bars in Atkinson and Boore (2006) gives results roughly comparable to what would have been obtained with a stress drop of 250 bars if a different normalization had been used. Thus, the higher stress drop of 250 bars is only applicable to the revised normalization scheme and not to the Atkinson and Boore (2006) equations. The Atkinson and Boore (2006) equations are correct as published and we do not intend to revise them on the basis of this article.

### Data and Resources

The stochastic point-source and stochastic finite-source modeling programs used in this article are SMSIM and

EXSIM, respectively. The versions used in this article are both freely accessible through David M. Boore's home page at [http://quake.usgs.gov/~boore/software\\_online.htm](http://quake.usgs.gov/~boore/software_online.htm). EXSIM, and ongoing improvements to the code, are also available at Dariush Motazedian's web site at <http://www.carleton.ca/~dariush/research/research.html>.

### References

- Aki, K. (1967). Scaling law of seismic spectrum, *J. Geophys. Res.* **72**, 1217–1231.
- Anderson, J. G., and S. E. Hough (1984). A model for the shape of the Fourier amplitude spectrum of acceleration at high frequencies, *Bull. Seismol. Soc. Am.* **74**, 1969–1993.
- Atkinson, G. (2004). Empirical attenuation of ground motion spectral amplitudes in southeastern Canada and the northeastern United States, *Bull. Seismol. Soc. Am.* **94**, 1079–1095.
- Atkinson, G. M., and I. Beresnev (1997). Don't call it stress drop, *Seism. Res. Lett.* **68**, 3–4.
- Atkinson, G. M., and D. M. Boore (1995). Ground motion relations for eastern North America, *Bull. Seismol. Soc. Am.* **85**, 17–30.
- Atkinson, G. M., and D. M. Boore (1997). Some comparisons between recent ground-motion relations, *Seism. Res. Lett.* **68**, 24–40.
- Atkinson, G. M., and D. M. Boore (2006). Earthquake ground-motion prediction equations for eastern North America, *Bull. Seismol. Soc. Am.* **96**, 2181–2205.
- Atkinson, G., and M. Macias (2009). Predicted ground motions for great interface earthquakes in the Cascadia subduction zone, *Bull. Seismol. Soc. Am.* **99**, no. 3, 1552–1578.
- Atkinson, G. M., and W. Silva (1997). An empirical study of earthquake source spectra for California earthquakes, *Bull. Seismol. Soc. Am.* **87**, 97–113.
- Atkinson, G. M., and W. Silva (2000). Stochastic modeling of California ground motions, *Bull. Seismol. Soc. Am.* **90**, 255–274.
- Beresnev, I. A., and G. M. Atkinson (1997). Modeling finite-fault radiation from the omega (super n) spectrum, *Bull. Seismol. Soc. Am.* **87**, 67–84.
- Beresnev, I. A., and G. M. Atkinson (1998a). FINSIM—A FORTRAN program for simulating stochastic acceleration time histories from finite faults, *Seism. Res. Lett.* **69**, 27–32.
- Beresnev, I. A., and G. M. Atkinson (1998b). Stochastic finite-fault modeling of ground motions from the 1994 Northridge, California, earthquake; I. Validation on rock sites, *Bull. Seismol. Soc. Am.* **88**, 1392–1401.
- Boore, D. M. (1983). Stochastic simulation of high-frequency ground motions based on seismological models of the radiated spectra, *Bull. Seismol. Soc. Am.* **73**, 1865–1894.
- Boore, D. M. (2000). SMSIM; Fortran programs for simulating ground motions from earthquakes; version 2.0, *U.S. Geol. Surv. Open-File Rept. 00-509*, 55.
- Boore, D. M. (2003). Simulation of ground motion using the stochastic method; Seismic motion, lithospheric structures, earthquake and volcanic sources; the Keiiti Aki volume, *Pure Appl. Geophys.* **160**, 635–676.
- Boore, D. M. (2005). SMSIM; Fortran programs for simulating ground motions from earthquakes: Version 2.3 A revision of OFR 96-80-A, *U.S. Geol. Surv. Open-File Rept.* (a modified version of OFR 00-509, describing the program as of 15 August 2005 [version 2.30]).
- Boore, D. M. (2009). Comparing stochastic point-source and finite-source ground-motion simulations: SMSIM and EXSIM, *Bull. Seismol. Soc. Am.* **99**, no. 6, 3202–3216.
- Boore, D. M., and G. M. Atkinson (1987). Stochastic prediction of ground motion and spectral response parameters at hard-rock sites in eastern North America, *Bull. Seismol. Soc. Am.* **77**, 440–467.

- Bour, M., and M. Cara (1997). Test of a simple empirical Green's function method on moderate-sized earthquakes, *Bull. Seismol. Soc. Am.* **87**, 668–683.
- Campbell, K. (2008). Hybrid empirical ground motion model for PGA and 5% damped linear elastic response spectra from shallow crustal earthquakes in stable continental regions: Example for eastern North America, *Proc. 14th World Conf. Earthq. Eng.*, Beijing, China, 12–17 October, Paper S03-001.
- Hanks, T. C., and J. Boatwright (1982). (Super F) Max; Special papers on the dynamic characteristics of faulting inferred from recordings of strong ground motion, *Bull. Seismol. Soc. Am.* **72**, 1867–1879.
- Hanks, T. C., and R. K. McGuire (1981). The character of high-frequency strong ground motion, *Bull. Seismol. Soc. Am.* **71**, 2071–2095.
- Hartzell, S. H. (1978). Earthquake aftershocks as Green's functions, *Geophys. Res. Lett.* **5**, 1–4.
- Irikura, K. (1983). Semi-empirical estimation of strong ground motions during large earthquakes, *Bull. Disast. Prev. Res. Inst.* **33**, 63–104.
- Irikura, K. (1992). The construction of large earthquake by a superposition of small events, *Proc. of the 10th World Conf. on Earthquake Engineering*, 727–730.
- Irikura, K., and K. Kamae (1994). Estimation of strong ground motion in broad-frequency band based on a seismic source scaling model and an empirical Green's function technique; Earthquake source mechanics, *Ann. Geophys.* **37**, 1721–1743.
- Macias, M., G. M. Atkinson, and D. Motazedian (2008). Ground-motion attenuation, source, and site effects for the 26 September 2003M 8.1 Tokachi–Oki earthquake sequence, *Bull. Seismol. Soc. Am.* **98**, 1947–1963.
- Motazedian, D. (2002). Development of earthquake ground motion relations for Puerto Rico, *Ph.D. Thesis*, Carleton University, Ottawa, Ontario, Canada.
- Motazedian, D., and G. M. Atkinson (2005). Stochastic finite-fault modeling based on a dynamic corner frequency, *Bull. Seismol. Soc. Am.* **95**, 995–1010.
- Toro, G. R., N. A. Abrahamson, and J. F. Schneider (1997). Model of strong ground motions from earthquakes in central and eastern North America; best estimates and uncertainties, *Seism. Res. Lett.* **68**, 41–57.

University of Western Ontario  
Department of Earth Sciences  
London, Ontario N6A 5B7  
gmatkinson@aol.com  
kassastou@uwo.ca  
(G.M.A., K.A.)

U.S. Geological Survey  
345 Middlefield Road  
Menlo Park, California 94025  
boore@usgs.gov  
(D.M.B.)

EQECAT, Inc.  
1030 NW 161st Place  
Beaverton, Oregon 97006  
KCampbell@eqecat.com  
(K.C.)

Carleton University  
Department of Earth Sciences  
Ottawa, Ontario K1S 5B6  
dariush\_motazedian@carleton.ca  
(D.M.)

Manuscript received 26 February 2009